IN 94

WL-EMP-IN-94

SC-TM-71 0319

THE RESPONSE OF AN ARBITRARILY TERMINATED WIRE NEAR THE SIDE OF A CONDUCTING CYLINDER

thin wires, conductors, cylinders, effects of EMP

Leonard D. Licking
Electromagnetics Effects Division, 1426
Sandia Laboratories
Albuquerque, New Mexico 87115

Date Published
July 1971

Key Word: Antennas

CONTENTS

	Page
1. INTRODUCTION	5
2. METHOD OF SOLUTION	6
3. FORMULATION	7
4. RESULTS	12
5. COMPARISON TO EXPERIMENTAL RESULTS	16
6. CONCLUSION	17
APPENDIX - NORMALIZATION AND TRANSIENT RESULTS	23

ILLUSTRATIONS

Figure		
1	Model of the missile system.	18
2	Geometry of model to be used for calculating the spatial phase change of $\bar{E}_{inc}$.	19
3	Graph of $\lvert cA_1(\epsilon, \varphi, z)/\epsilon \rvert = \lvert cA_1(z)/\epsilon \rvert$.	20
4	Comparison of experimental and theoretical results.	21

The Response of an Arbitrarily Terminated Wire Near the Side of a Conducting Cylinder

Leonard D. Licking
Sandia Laboratories
Albuquerque, New Mexico 87115

ABSTRACT

A perfectly conducting cylinder which has a wire running parallel to its axis and very close to its surface is assumed to be illuminated by a plane wave electromagnetic field. Formulas for the currents in arbitrary loads which connect the ends of the wire to the cylinder are presented.

1. INTRODUCTION

Many missile systems have been designed with external cables which run parallel to the axis of the missile and very close to the missile skin. These cables may be able to transmit significant amounts of energy to internal electronic packages when the structure is illuminated by an electromagnetic field. To be able to predict whether the missile will function properly after exposure to electromagnetic fields, one must be able to determine the currents and voltages induced inside the missile.

This problem has been previously addressed by Harrison [1967]; however, his analysis neglected the radial electric fields at the ends of the cable. In this paper, it is shown that these radial fields are major contributors to the total system response and must not be neglected.

For this analysis the missile and cable will be modeled by a perfectly conducting cylinder and a parallel wire that is connected to the cylinder through arbitrary impedances at each end of the wire (Figure 1). The cylinder has a half-length of h and a radius of a; the wire has a length of ℓ and a radius of a_1; and the bottom termination of the wire is located a distance g from the center of the cylinder ($g < 0$ if the bottom connection is below the center of the cylinder). The minimum distance from the cylinder skin to the center of the wire is ϵ; the angle formed by the positive x axis and the line which connects the axis of the cylinder to the axis of the wire is ψ. The incident field is assumed to be a plane wave which propagates in the positive x direction, is polarized in the z direction, and has an electric field of magnitude $E_0 = |\bar{E}_{inc}|$.

2. METHOD OF SOLUTION

As in the procedure of Harrison [1967], the wire and its image in the perfectly conducting cylinder will be treated as a transmission line that is excited by that component of the electric field which is tangent to the wire and its image electric field in the cylinder. The electric field to be considered here is the incident field plus the scattered field from the cylinder. Both axial and radial fields near the cylinder must be found, since the tangent to the wire is in the radial direction at the ends of the wire.

Note that this procedure accounts for the effects on the wire due to the presence of the cylinder, but the effects on the cylinder due to the presence of the wire

are neglected. This approximation should have little effect on the answer, since the volume of space occupied by the cylinder is much greater than that of the wire.

The response I(z) of a transmission line when driven by a distributed voltage source V(z) is given by

$$I(z) = \int_g^{g+\ell} G(z, z')V(z')\, dz' \,. \tag{1}$$

Here, G(z, z') is the appropriate Green's function for a transmission line. For this problem, V(z') is that component of the electric field tangent to the wire.

3. FORMULATION

When the cylinder is illuminated by an incident plane wave with time variations of the form $e^{j\omega t}$, the scattered field at the point (r, φ, z) is

$$\bar{E}_s(r, \varphi, z) = \bar{E}_0\left[-j\omega\bar{A} + \frac{1}{j\omega\mu_0\epsilon_0}\nabla(\nabla \cdot \bar{A})\right] \,. \tag{2}$$

Here,

$$\bar{A}(r, \varphi, z) = \frac{\mu_0 a}{4\pi}\int_{-h}^{h}\int_0^{2\pi} \bar{J}(\varphi', z')\,\frac{e^{-jk_0R}}{R}\, d\varphi'\, dz' \tag{3}$$

and

$$R = \sqrt{(z - z')^2 + r^2 + a^2 - 2ar\cos(\varphi - \varphi')} \,, \tag{4}$$

where $k_0 = \omega/c$, and $\bar{J}(\varphi', z')$ is the current density on the cylinder due to a unit incident electric field.

Since the incident electric field is parallel to the axis of the cylinder

$$\bar{E}_{inc}(a + \epsilon, \psi, z) = -E_{sz}(a, \psi, z)\, e^{-jk_0\epsilon\cos\psi}\,\bar{a}_z \,, \tag{5}$$

where E_{sz} is the z component of $\bar{E}_s$, $-h \le z \le h$, and $\bar{a}_z$ is a unit vector in the z direction (see Figure 2). The total electric field is the sum of $\bar{E}_{inc}$ and $\bar{E}_s$. The total electric field near the wire (with the wire removed) is

$$\bar{E}_t(a+\epsilon, \psi, z) = \frac{-j\omega E_0}{k_0^2}\left[k_0^2\left\{\bar{A}(a+\epsilon, \psi, z) - A_z(a, \psi, z)\, e^{-jk_0\epsilon\cos\psi}\,\bar{a}_z\right\}\right.$$

$$+\left\{\frac{\partial}{\partial r}(\nabla\cdot\bar{A})\bar{a}_r + \frac{1}{r}\frac{\partial}{\partial\varphi}(\nabla\cdot\bar{A})\bar{a}_\varphi + \frac{\partial}{\partial z}(\nabla\cdot\bar{A})\bar{a}_z\right\}_{\substack{r=a+\epsilon\\ \varphi=\psi}}$$

$$\left.-\left(\frac{\partial}{\partial z}(\nabla\cdot\bar{A})\right)_{\substack{r=a\\ \varphi=\psi}} e^{-jk_0\epsilon\cos\psi}\,\bar{a}_z\right] \cdot \qquad (6)$$

Along the wire, the distributed voltage source V(z) is the tangential component of $\bar{E}_t(a+\epsilon, \psi, z)$; that is,

$$V(z) = 2\left[E_{tz}(a+\epsilon, \psi, z) + \left\{\int_a^{a+\epsilon} E_{tr}(r, \psi, z)\, dr\right\}\{\delta(z-g) - \delta(z-\ell-g)\}\right] \cdot \qquad (7)$$

In (7), E_{tz} and E_{tr} are the z and r components of E_t, $\delta(z)$ is the Dirac delta function, and the factor of two is due to the image electric field in the cylinder. Equations (6) and (7) yield

$$V(z) = -\frac{2j\omega E_0}{k_0^2}\left[k_0^2\left\{A_z(a+\epsilon, \psi, z) - A_z(a, \psi, z)\, e^{-jk_0\epsilon\cos\psi}\right\}\right.$$

$$+\frac{\partial}{\partial z}(\nabla\cdot\bar{A})\Big|_{\substack{r=a+\epsilon\\ \varphi=\psi}} - \frac{\partial}{\partial z}(\nabla\cdot\bar{A})\Big|_{\substack{r=a\\ \varphi=\psi}} e^{-jk_0\epsilon\cos\psi}$$

$$\left.+\left\{k_0^2\int_a^{a+\epsilon} A_r(r, \psi, z)\, dr + \nabla\cdot\bar{A}\Big|_{r=a+\epsilon} - \nabla\cdot\bar{A}\Big|_{r=a}\right\}_{\varphi=\psi}\right.$$

$$\{\delta(z - g) - \delta(z - g - \ell)\}\Big]$$

$$= -\frac{2j\omega E_0}{k_0^2}\Bigg[k_0^2\Big\{A_z(a + \epsilon, \psi, z) - A_z(a, \psi, z)\Big\} + \frac{\partial}{\partial z}\Big\{\nabla \cdot \bar{A}\big|_{r=a+\epsilon} - \nabla \cdot \bar{A}\big|_{r=a}\Big\}_{\varphi=\psi}$$

$$+ \Big\{k_0^2 \int_a^{a+\epsilon} A_r(r, \psi, z)\, dr + \nabla \cdot \bar{A}\big|_{r=a+\epsilon} - \nabla \cdot \bar{A}\big|_{r=a}\Big\}_{\varphi=\psi}$$

$$\{\delta(z - g) - \delta(z - g - \ell)\}$$

$$+ \Big\{k_0^2 A_z(a, \varphi, z) + \frac{\partial}{\partial z}\nabla \cdot \bar{A}\Big\}_{\substack{r=a \\ \varphi=\psi}}\Big\{1 - e^{-jk_0\epsilon \cos \psi}\Big\}\Bigg]$$

$$= \frac{-2j\omega E_0}{k_0^2}\left[k_0^2 A_1 + \frac{\partial F}{\partial z} + \Big\{k_0^2 \int_a^{a+\epsilon} A_r(r, \psi, z)\, dr + F\Big\}\{\delta(z - g) - \delta(z - g - \ell)\}\right]$$

$$-2\bar{E}_{inc}(a, \psi, z) \cdot \bar{a}_z\Big\{1 - e^{-jk_0\epsilon \cos \psi}\Big\} \quad . \tag{8}$$

Here,

$$A_1(\epsilon, \psi, z) = A_z(a + \epsilon, \psi, z) - A_z(a, \psi, z)$$

$$= \frac{\mu_0 a}{4\pi}\int_{-h}^{h}\int_0^{2\pi}\left(\frac{e^{-jk_0R_1}}{R_1} - \frac{e^{-jk_0R_2}}{R_2}\right)J_z(\varphi', z')\, d\varphi'\, dz' \,, \tag{9}$$

$$R_1 = R\big|_{\substack{r=a+\epsilon \\ \varphi=\psi}}, \quad R_2 = R\big|_{\substack{r=a \\ \varphi=\psi}}, \quad g \le z,\ z' < g + \ell,$$

and

$$F = \nabla \cdot \bar{A}\big|_{\substack{r=a+\epsilon \\ \varphi=\psi}} - \nabla \cdot \bar{A}\big|_{\substack{r=a \\ \varphi=\psi}} \quad . \tag{10}$$

If the φ component of $\bar{J}$ is negligible, (8) can be written

$$V(z) = \frac{-2E_0 j\omega}{k_0^2}\left[k_0^2 A_1(\epsilon,\ \psi,\ z) + \frac{\partial^2}{\partial z^2} A_1(\epsilon,\ \psi,\ z)\right.$$

$$\left. + \frac{\partial}{\partial z} A_1(\epsilon,\ \psi,\ z)\{\delta(z - g) - \delta(z - g - \ell)\}\right] - E_0\left\{1 - e^{-jk_0\epsilon\cos\psi}\right\} . \quad (11)$$

The Green's function for current when the transmission line is driven by a voltage source is

$$G(z,\ z') = \begin{cases} \dfrac{e^{jk_0(z-z')}\left(1 - \rho_\ell e^{j2k_0(z'-g-\ell)}\right)\left(1 - \rho_g e^{-j2k_0(z-g)}\right)}{2Z_c\left(1 - \rho_g\rho_\ell e^{-j2k_0\ell}\right)}, & g \le z < z' \le g + \ell \\ \dfrac{e^{jk_0(z'-z)}\left(1 - \rho_\ell e^{j2k_0(z-g-\ell)}\right)\left(1 - \rho_g e^{-j2k_0(z'-g)}\right)}{2Z_c\left(1 - \rho_g\rho_\ell e^{-j2k_0\ell}\right)}, & g \le z' < z \le g + \ell. \end{cases} \quad (12)$$

Here,

$$\rho_g = \frac{2Z_g - Z_c}{2Z_g + Z_c} , \quad (13)$$

$$\rho_\ell = \frac{2Z_\ell - Z_c}{2Z_\ell + Z_c} , \quad (14)$$

and

$$Z_c = 120\ell n\left[\epsilon/a_1 + \sqrt{(\epsilon/a_1)^2 - 1}\right] \tag{15}$$

= the characteristic impedance of the line

(the wire and its image).

In (13) and (14) two times the terminating impedances are used because of their images in the cylinder.

Substituting (11) and (12) into (1), integrating by parts (twice where necessary), and evaluating the result at $z = g$ and $z = g + \ell$ yields the currents in Z_g and Z_ℓ. The results are

$$I_g = \frac{-(1 - \rho_g)E_0}{Z_c\left(1 - \rho_g\rho_\ell\, e^{-j2k_0\ell}\right)}\left\{c\, e^{-jk_0\ell}\left[A_1(\epsilon, \psi, g)\left(e^{jk_0\ell} + \rho_\ell\, e^{-jk_0\ell}\right)\right.\right. \tag{16}$$

$$\left.\left. - (1 + \rho_\ell)A_1(\epsilon, \psi, g + \ell)\right] + \left(1 - e^{-jk_0\epsilon\cos\psi}\right)\left(1 - e^{-jk_0\ell}\right)\left(1 - \rho_\ell\, e^{-jk_0\ell}\right)\Big/jk_0\right\}$$

and

$$I_\ell = \frac{-(1 - \rho_\ell)E_0}{Z_c\left(1 - \rho_g\rho_\ell\, e^{-j2k_0\ell}\right)}\left\{c\, e^{-jk_0\ell}\left[A_1(\epsilon, \psi, g + \ell)\left(e^{jk_0\ell} + \rho_g\, e^{-jk_0\ell}\right)\right.\right. \tag{17}$$

$$\left.\left. - (1 + \rho_g)A_1(\epsilon, \psi, g)\right] + \left(1 - e^{-jk_0\epsilon\cos\psi}\right)\left(1 - e^{-jk_0\ell}\right)\left(1 - \rho_g\, e^{-jk_0\ell}\right)\Big/jk_0\right\}.$$

Equations (16) and (17) are formulas for the desired currents. Voltages can be found by multiplying (16) and (17) by the appropriate load impedances.

4. RESULTS

If the wire is shorted to the cylinder at both ends,

$$\rho_g = \rho_\ell = -1$$

and

$$I_{\ell sc} = -\frac{2E_0}{Z_c}\left[cA_1(\epsilon, \psi, g + \ell) + \left(1 - e^{-jk_0\epsilon \cos \psi}\right)\Big/jk_0\right] . \tag{18}$$

For $k_0 h \ll 1$, A_1 is proportional to ω and, therefore, $I_{\ell sc}$ is proportional to ω if $\cos \psi = 0$ or is constant with respect to ω if $\cos \psi \neq 0$; that is,

$$I_{\ell sc} = C_1 \omega \text{ if } \cos \psi = 0 \tag{19}$$

or

$$I_{\ell sc} = C_2 \text{ if } \cos \psi \neq 0 . \tag{20}$$

C_1 and C_2 do not depend on ω. For $\rho_g = \rho_\ell = -1$ and $k_0 h \ll 1$, equation 50 from Harrison [1967] reduces to the form

$$I_{\ell sc} = C_3/\omega . \tag{21}$$

The difference between (21) and (19) is due to the radial fields near the ends of the wire.

Examination of (11) shows why the radial fields cannot be neglected. In (11), if $k_0 h \ll 1$, the term

$$\left(\omega/k_0^2\right)\frac{\partial^2}{\partial z^2} A_1(\epsilon, \psi, z)$$

is constant, ωA_1 varies as ω^2, and

$$\left(1 - e^{-jk_0 \epsilon \cos \psi}\right)$$

varies as ω. Therefore,

$$\left(\omega/k_0^2\right)\frac{\partial^2}{\partial z^2} A_1(\epsilon, \psi, z)$$

is the dominant term in (11) except at $z = g$ or $g + \ell$. The term

$$\left(\omega/k_0^2\right) \frac{\partial}{\partial z} A_1(\epsilon, \psi, z)\left[\delta(z - g) - \delta(z - g - \ell\right]$$

is a result of the radial field at the ends of the wire. Integration of these two terms along the wire yields

$$\int_g^{g+\ell} \frac{\partial^2}{\partial z^2} A_1(\epsilon, \psi, z)\, dz + \int_g^{g+\ell} \frac{\partial}{\partial z} A_1(\epsilon, \psi, z)\left[\delta(z - g) - \delta(z - g - \ell)\right] dz$$

$$= \frac{\partial}{\partial z} A_1(\epsilon, \psi, z)\Big|_{z=g}^{z=g+\ell} - \frac{\partial}{\partial z} A_1(\epsilon, \psi, z)\Big|_{z=g}^{z=g+\ell} = 0 . \quad (22)$$

Equation (22) shows that the dominant part of the integral of the z component of the electric field along the wire is the negative of the integral of the radial

component of the electric field at the ends of the wire. The net effect is that these two terms tend to cancel each other and that the remaining terms in (11) are the dominant terms.

Each of the two terms of (18) has a distinct physical interpretation. Let

$$I_{\ell sc} = I_{\ell sc1} + I_{\ell sc2} \tag{23}$$

where

$$I_{\ell sc1} = -\frac{2E_0}{Z_c} cA_1(\epsilon, \psi, g + \ell) \tag{24}$$

and

$$I_{\ell sc2} = -\frac{2E_0}{Z_c}\left(1 - e^{-jk_0\epsilon\cos\psi}\right)\Big/jk_0 \cdot \tag{25}$$

Equation (9) shows that $A_1(\epsilon, \psi, z)$ is dependent on the current density on the cylinder; in fact, $A_1(\epsilon, \psi, z)$ is nearly proportional to the product of ϵ and the current density at the point (a, ψ, z). Through use of available current distributions on a cylinder [Harrison et al., 1967], (9) was evaluated numerically for A_1. The current distribution program of Harrison et al. [1967] neglects the effects of shadowing so that J_z is independent of φ. Therefore, in this calculation, A_1 was not a function of ψ. Numerical results show that A_1 is proportional to ϵ. The shape of the graph of $A_1(z_1)/\epsilon$ versus k_0h (Figure 3) confirms that A_1, and therefore $I_{\ell sc1}$, is nearly proportional to the total current on the cylinder at $z = z_1$. Here, $A_1(\epsilon, \psi, z)$ was written as $A_1(z)$ to emphasize that $A_1(\epsilon, \psi, z)$ is independent of ψ and nearly proportional to ϵ when shadowing is neglected.

$I_{\ell sc2}$ is a result of the second term of (8), which is

$$V_2(z') = -2E_0\left(1 - e^{-jk_0\epsilon\cos\psi}\right) . \tag{26}$$

Since $k_0\epsilon \ll 1$, for all frequencies of interest

$$V_2(z') = -2jE_0k_0\epsilon\cos\psi = -j\omega 2\Phi_{inc} , \tag{27}$$

where Φ_{inc} is the magnetic flux per unit length due to the incident field which is enclosed by the wire and the cylinder skin. Thus, (25) is an equation for that part of the current due to the derivative with respect to time of the enclosed magnetic flux of the incident field.

Note that the short-circuit current is independent of the length of the wire and has no resonant frequencies corresponding to the length of the transmission line (wire). The lack of resonant frequencies is due to the distributed source V(z).

A numerical calculation will give an indication of the currents which can be expected. Consider a missile system with the following parameters: h = 5 m, a = 0.5 m, $a_1 = 2.5 \times 10^{-3}$ m, $g + \ell = 0$, $\epsilon = 10^{-2}$ m, and $\psi = \pi$. Let the incident electric field have a magnitude of 1 volt/m and a frequency of 10 MHz. Then, $Z_c = 247.6$ ohms and $k_0h = 0.955$. Using Figure 3 gives

$$|I_{\ell sc1}| = 1 \times \frac{2 \times 10^{-2}}{247.6} \times 7.1$$

$$= 5.7 \times 10^{-4} \text{ amps} ,$$

$$|I_{\ell sc1}| = 1 \times \frac{2}{247.6} \times 10^{-2}$$

$$= 8.1 \times 10^{-5} \text{ amps},$$

and

$$|I_{\ell sc}| \approx 6.5 \times 10^{-4} \text{ amps}.$$

Multiplication of these currents by the high-magnitude electric fields due to EMP or lightning would result in a significant amount of short-circuit current.

5. COMPARISON TO EXPERIMENTAL RESULTS

An experimental model was mounted on a large metal ground plane and illuminated by an electromagnetic field. The model and its image in the metal ground plane form the free space equivalent of the structure analyzed in this report. Parameters of the system had the following values: $h = \ell = 0.191$ m, $a = 9.5 \times 10^{-3}$ m, $a_1 = 4.1 \times 10^{-4}$ m, $\epsilon = 1.22 \times 10^{-3}$ m, $Z_g = Z_\ell = 50$ ohms, and $\psi = \pi/2$ and π.

Inasmuch as (23), (24), and (25) can be generalized to include cases where the wire is not shorted to the cylinder, I_ℓ can be expressed as

$$I_\ell = I_{\ell 1} + I_{\ell 2}. \tag{26}$$

If $\psi = \pi/2$, then $I_{\ell 2} = 0$ and no magnetic flux from the incident field is enclosed by the wire and the cylinder skin. Figure 4a shows graphs of experimental and theoretical values of current in the 50-ohm resistor, Z_ℓ. If $\psi = \pi$, neither $I_{\ell 1}$ nor $I_{\ell 2}$ is zero and both terms of (26) must be used. If $k_0 h \leq 0.2$, $|I_{\ell 2}| \gg |I_{\ell 1}|$ so that $|I_\ell| \simeq |I_{\ell 2}|$ on the left side of Figure 4b and if $0.5 \leq k_0 h \leq 10$,

$|I_{\ell 1}| \gg |I_{\ell 2}|$ so that $|I_\ell| \simeq |I_{\ell 1}|$ on the right side of Figure 4b. Thus, the transition region where both $I_{\ell 1}$ and $I_{\ell 2}$ make significant contributions to I_ℓ is included in Figure 4b.

6. CONCLUSION

A method for calculating currents and voltages induced in the loads of a cylinder and parallel wire configuration has been presented. Shadowing effects have been neglected in the numerical results. Since $A_1(\varepsilon, \psi, z)$ is nearly proportional to the current density on the cylinder at the point (a, ψ, z), the high-frequency portion of Figure 3 would be too small if the wire was on the illuminated side of the cylinder and would be too large if it was on the shadowed side. $I_{\ell sc2}$ would not be affected by shadowing.

If the incident electric field was not polarized in the z direction, the results of this paper could be applied by defining E_0 as $E_0 = |\bar{E}_{inc} \cdot \bar{a}_z|$ instead of $E_0 = |\bar{E}_{inc}|$. Since J_φ is altered by the y component of $\bar{E}_{inc}$, the assumption that the effects due to J_φ are negligible may become less valid and, therefore, introduce some error in the results.

It is possible that (6) could be used to calculate the electric fields near a cylinder when illuminated by a plane wave. However, the derivatives in (6) would have to be taken numerically after the integrals for A were evaluated, because the derivative and integral signs cannot be interchanged when r = a.

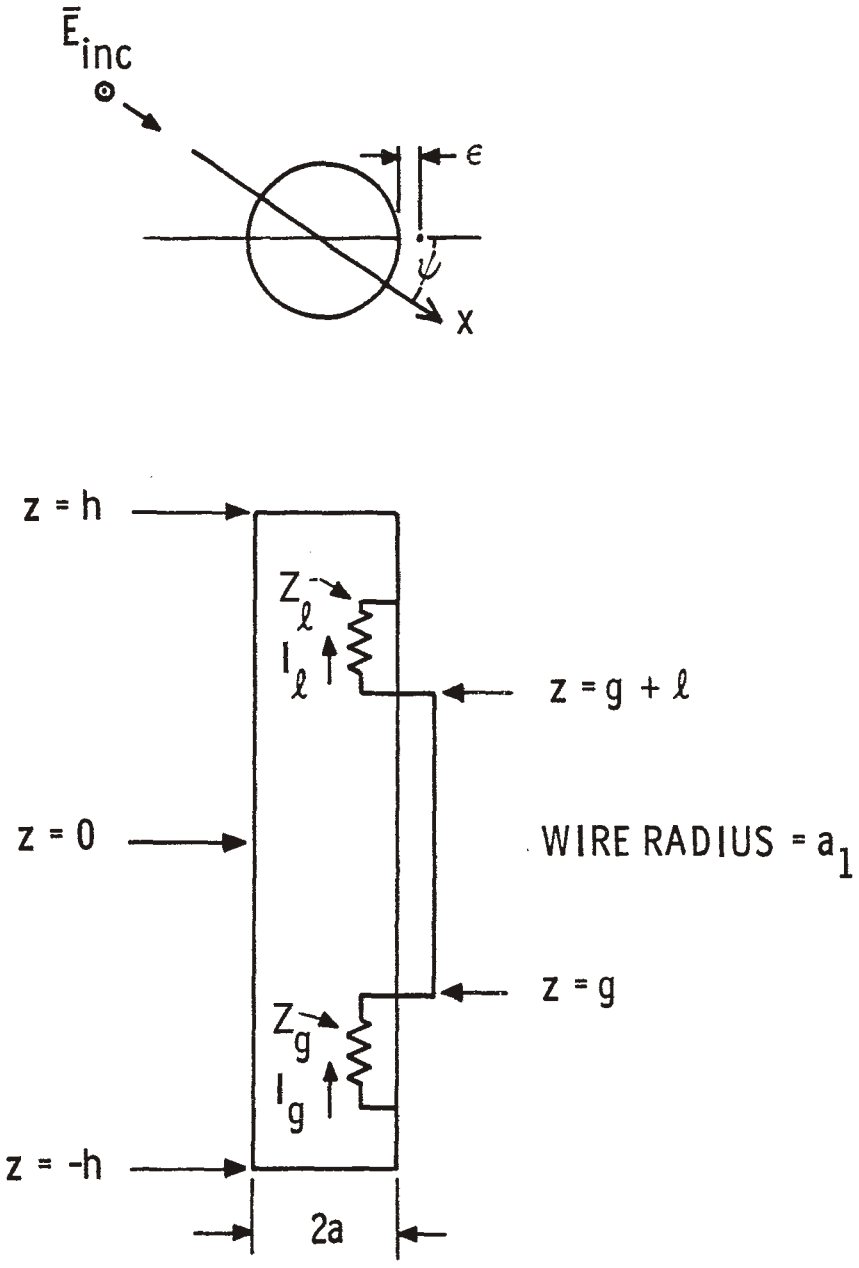

Fig. 1. Model of the missile system.

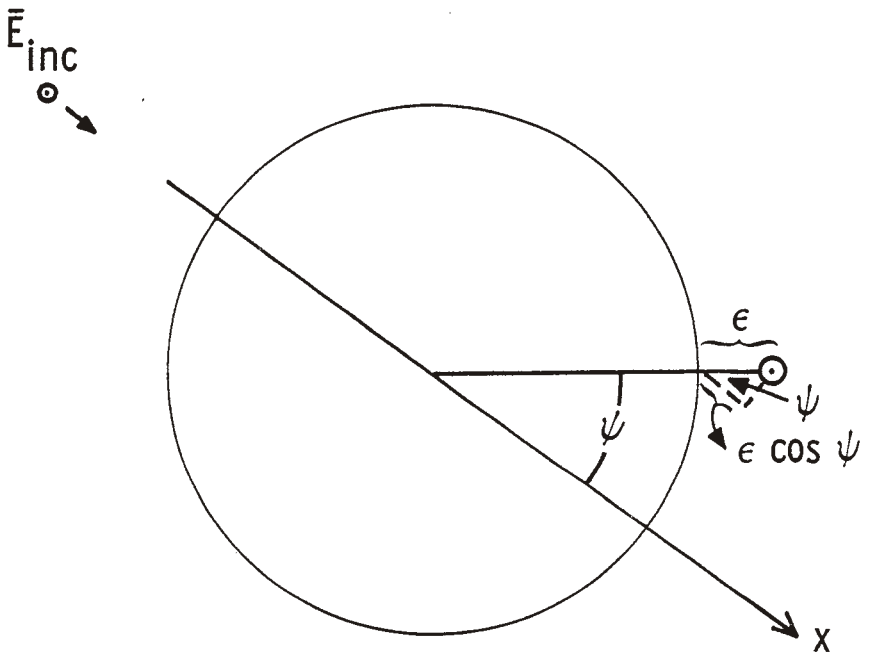

Fig. 2. Geometry of model to be used for calculating the spatial phase change of $\bar{E}_{inc}$.

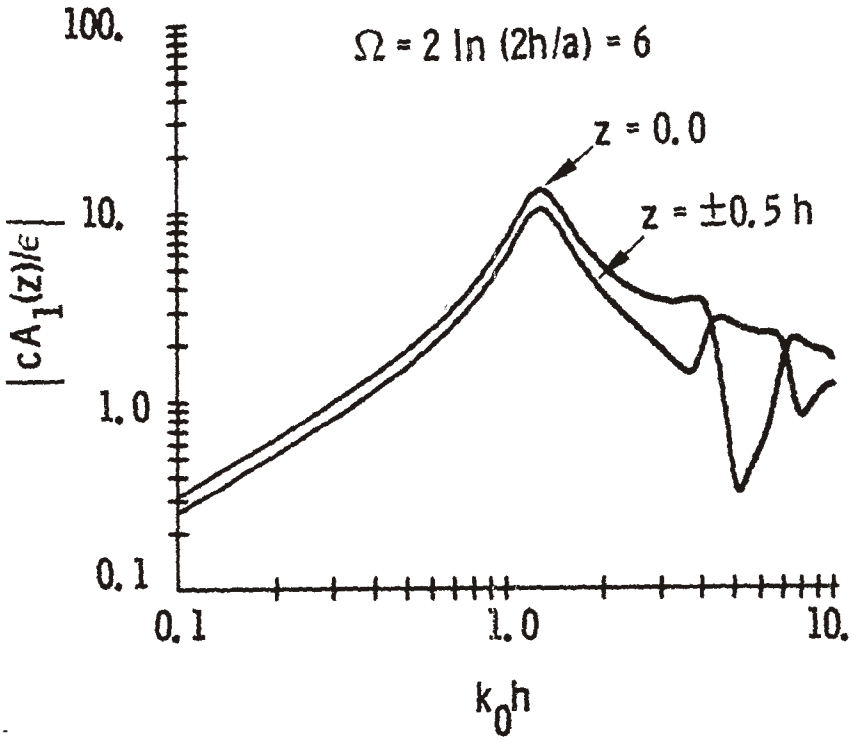

Fig. 3. Graph of $|cA_1(\epsilon, \varphi, z)/\epsilon| = |cA_1(z)/\epsilon|$.

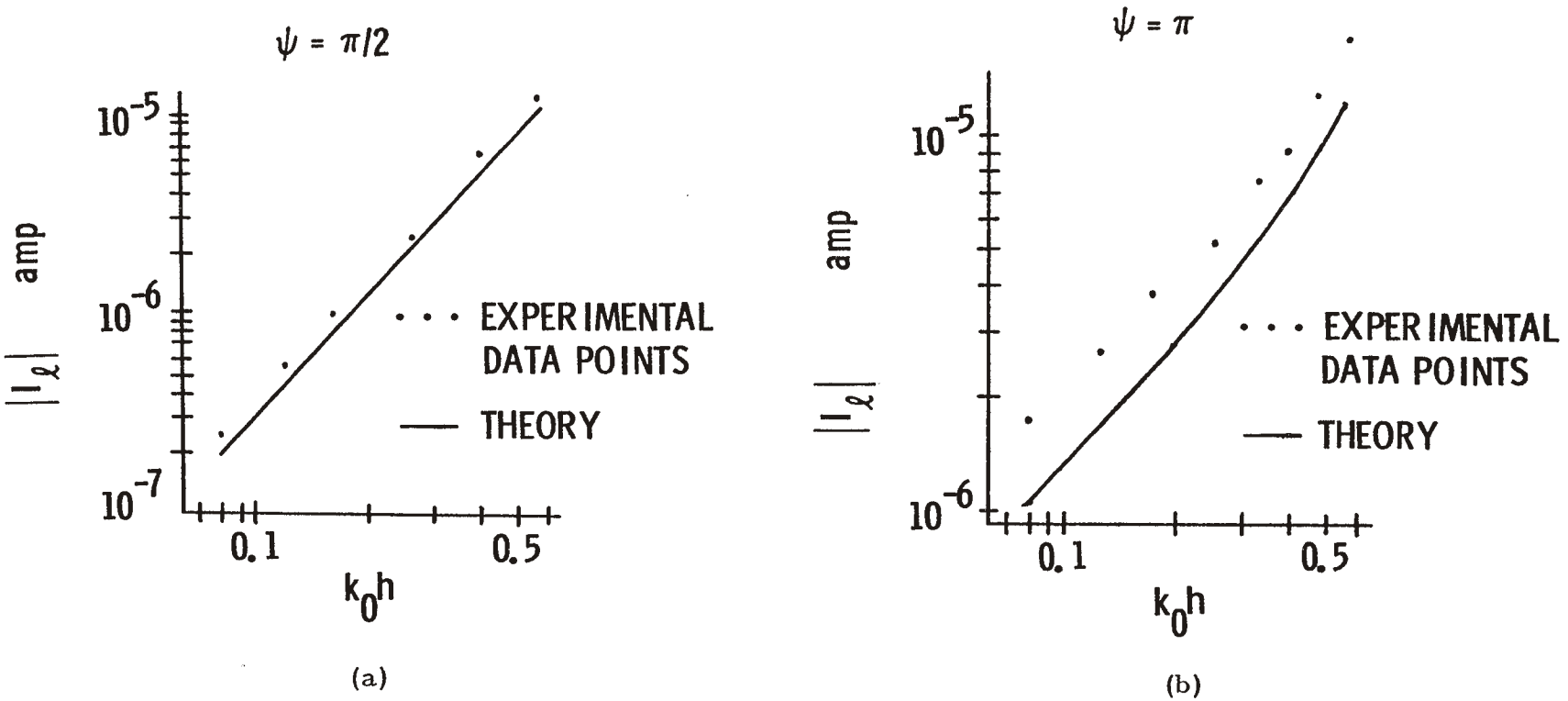

Fig. 4. Comparison of experimental and theoretical results.

APPENDIX

NORMALIZATION AND TRANSIENT RESULTS

As shown in section 4, the currents in Z_g and Z_ℓ can be broken into two parts. One part can be normalized with respect to the cylinder parameters and the other part cannot be so normalized. However, the part that cannot be normalized can be expressed by an algebraic formula making normalization unnecessary.

From (17) the two parts of I_ℓ are

$$I_{\ell 1} = \frac{-(1 - \rho_\ell)E_0}{Z_c\left(1 - \rho_g\rho_\ell\, e^{-j2k_0\ell}\right)} c\, e^{-jk_0\ell}\left\{A_1(\epsilon,\ \psi,\ g + \ell)\left(e^{jk_0\ell} + \rho_g\, e^{-jk_0\ell}\right)\right.$$

$$\left. - (1 + \rho_g)A_1(\epsilon,\ \psi,\ g)\right\} \qquad \text{(A. 1)}$$

and

$$I_{\ell 2} = \frac{-(1 - \rho_\ell)E_0}{Z_c\left(1 - \rho_g\rho_\ell\, e^{-j2k_0\ell}\right)}\left(1 - e^{-jk_0\epsilon\cos\psi}\right)\left(1 - e^{-jk_0\ell}\right)$$

$$\left(1 - \rho_g\, e^{-jk_0\ell}\right)\Big/jk_0 \ . \qquad \text{(A. 2)}$$

Normalization

Equation (A. 1) can be normalized by the following procedure. From (9),

$$A_1(\varepsilon, \psi, z) = \frac{\mu_0}{8\pi^2} \int_{-h}^{h} \int_0^{2\pi} \frac{e^{-jk_0R_1}}{R_1} - \frac{e^{-jk_0R_2}}{R_2} d\varphi' I(z') dz' . \quad (A.3)$$

Here, it was assumed that J_z is a function of z only and that

$$I(z') = 2\pi a J_z(z') . \quad (A.4)$$

From Harrison et al. [1967], I(z') has the form

$$I(z') = hF_1(z'/h, \Omega) . \quad (A.5)$$

Here, $\Omega = 2\ell n(2h/a)$, and $F_1(x_1, x_2)$ is to be read as a function of x_1 and x_2. Using (4) it can be shown that

$$R_1 = hF_2[(z - z')/h, \varepsilon/h, \Omega, (\varphi - \varphi')] \quad (A.6)$$

and

$$R_2 = hF_3[(z - z')/h, \Omega, (\varphi - \varphi')] . \quad (A.7)$$

Substituting (A. 5), (A. 6), and (A. 7) into (A. 3) and using the change of dummy variable $z_1 = z'/h$ shows that

$$cA_1(\varepsilon, \psi, z) = hF_4(z/h, \varepsilon/h, \Omega, k_0h) . \quad (A.8)$$

A_1 is not a function of φ because J_z was assumed to be independent of φ. Analysis of numerical results show that F_4 has the form

$$F_4(z/h, \varepsilon/h, \Omega, k_0h) = \frac{\varepsilon}{h} F_5(z/h, \Omega, k_0h) \quad (A.9)$$

over the range of values of ϵ/h of interest. Thus,

$$cA_1(\epsilon, \psi, z) = \epsilon F_5(z/h, \Omega, k_0 h) . \tag{A.10}$$

Equation (A.10) justifies the normalization procedure used in Figure 3. If the load impedances are resistive, ρ_g and ρ_ℓ are independent of ω and are not affected by normalization, because Z_c is not changed by normalization. Substituting (A.10) into (A.1) shows

$$I_{\ell 1} = \frac{2E_0\epsilon}{Z_c} F_6(g/h, \ell/h, \rho_g, \rho_\ell, \Omega, k_0 h) \tag{A.11}$$

for resistive loads. Equation (A.11) is the general normalized equation for $I_{\ell 1}$.

Short-Circuit Current - CW

If the wire is shorted to the cylinder at both ends, $\rho_g = \rho_\ell = -1$ and (A.1) and (A.2) become

$$I_{\ell 1} = \frac{-2cE_0}{Z_c} A_1(\epsilon, \psi, g + \ell)$$

$$= \frac{-2E_0}{Z_c} \epsilon F_5[(g + \ell)/h, \Omega, k_0 h] \tag{A.12}$$

and

$$I_{\ell 2} = \frac{-2E_0}{Z_c} \left(1 - e^{-jk_0\epsilon \cos \psi}\right) \Big/ jk_0 . \tag{A.13}$$

Open-Circuit Voltage - CW

If the wire is open circuited at $z = g + \ell$ and shorted to the cylinder at $z = g$, $\rho_g = -1$ and $\rho_\ell = 1$. Using (13), (14), (A. 1), and (A. 2) it can be shown that the two terms of the open-circuit voltage are

$$V_{\ell 0c1} = (j \tan k_0 \ell)\left[-E_0 c A_1(\epsilon, \psi, g + \ell)\right]$$

$$= (j \tan k_0 \ell)\left[-E_0 \epsilon F_5\left((g + \ell)/h, \Omega, k_0 h\right)\right] \qquad (A.14)$$

and

$$V_{\ell 0c2} = (j \tan k_0 \ell)\left[-E_0\left(1 - e^{-jk_0 \epsilon \cos \psi}\right)\Big/ jk_0\right]. \qquad (A.15)$$

Transient Analysis

Transient response is obtained by using either

$$r(t) = \frac{2}{\pi} \int_0^\infty \mathrm{Re}\left[E(\omega)T(\omega)\right] \cos \omega t \, d\omega, \quad t \geq 0 \qquad (A.16)$$

or

$$r(t) = -\frac{2}{\pi} \int_0^\infty \mathrm{Im}\left[E(\omega)T(\omega)\right] \sin \omega t \, d\omega, \quad t \geq 0 . \qquad (A.17)$$

Here, $r(t)$ is the transient signal, $E(\omega)$ is the Fourier transform of the incident electric field, and $T(\omega)$ is the CW transfer function.

The incident electric field will be assumed to be a step of magnitude, E_0, in the remaining portion of this report. Then

$$E(\omega) = \frac{E_0}{j\omega} \qquad (A.18)$$

and

$$R(t) = \frac{2E_0}{\pi} \int_0^\infty \mathrm{Im}[T(\omega)] \frac{\cos \omega t}{\omega} \, d\omega, \quad t \geq 0 \, . \tag{A.19}$$

Equations (A.11) and (A.19) show that (substitute $I_{\ell 1}$ for T)

$$i_{\ell 1}(t) = \frac{2E_0 \epsilon}{Z_c} f_6(g/h, \ \ell/h, \ \rho_g, \ \rho_\ell, \ \Omega, \ tc/h) \tag{A.20}$$

if the wire is terminated in resistive loads. Equation (A.20) is the general normalized equation for $i_{\ell 1}$. Figures A-1 through A-8 are plots of $f_6(g/h, \ \ell/h, \ \rho_g, \ \rho_\ell, \ \Omega, \ tc/h)$ versus tc/h for various values of the parameters g/h, ℓ/h, ρ_g, and ρ_ℓ. $\Omega = 6$ in all figures.

An algebraic formula for $i_{\ell 2}(t)$ will now be found.

Multiplication of (A.2) by (A.18) and rearranging yield

$$E(\omega) I_{\ell 2} = \frac{-(1 - \rho_\ell) c E_0}{Z_c}$$

$$\left[\frac{1 - e^{-j\omega p} - (1 + \rho_g)\left\{ e^{-j\omega q} - e^{-j\omega(p+q)} \right\} + \rho_g \left\{ e^{-j\omega 2q} - e^{-j\omega(p+2q)} \right\}}{(j\omega)^2} \right]$$

$$\left[\sum_{i=0}^{\infty} (\rho_g \rho_\ell)^i \, e^{-j\omega 2iq} \right]. \tag{A.21}$$

Here,

$$p = \frac{\epsilon \cos \Psi}{c} \tag{A.22}$$

and

$$q = \ell/c \, . \tag{A.23}$$

Multiplying (A.21) by the delay factor, $e^{-j\omega\epsilon/c}$, to force the signal to zero for $t < 0$ and inverse transforming (A.21) yield

$$i_{\ell 2}(t) = \frac{-(1 - \rho_\ell)cE_0}{Z_c} \sum_{i=0}^{\infty} (\rho_g \rho_\ell)^i f(t - 2iq) \tag{A.24}$$

where

$$\begin{aligned} f(t) = {} & (t - \epsilon/c)U(t - \epsilon/c) - (t - p - \epsilon/c)U(t - p - \epsilon/c) - (1 + \rho_g) \\ & \left[(t - q - \epsilon/c)U(t - q - \epsilon/c) - (t - p - q - \epsilon/c)U(t - p - q - \epsilon/c)\right] \\ & + \rho_g\left[(t - 2q - \epsilon/c)U(t - 2q - \epsilon/c) - (t - p - 2q - \epsilon/c)\right. \\ & \left. U(t - p - 2q - \epsilon/c)\right] . \end{aligned} \tag{A.25}$$

The current at $z = g + \ell$ is the sum of (A.20) and (A.24); that is,

$$i_\ell(t) = i_{\ell 1}(t) + i_{\ell 2}(t) \, .$$

If the wire is shorted to the cylinder at both ends, (A.26) and (A.24) assume simpler forms.

Short-Circuit Current - Transient Response to a Step Incident Field

Inverse transformation of (A.12) times (A.18) shows that $i_{\ell sc1}(t)$ has the form

$$i_{\ell sc1}(t) = \frac{\epsilon E_0}{Z_c} f_5\left((g + \ell)/h, \, \Omega, \, tc/h\right) . \tag{A.27}$$

Graphs of f_5 are shown in Figure A-9. For $\rho_g = \rho_\ell = -1$, (A.24) reduces to

$$i_{\ell sc2}(t) = \frac{2E_0 \epsilon \cos \psi}{Z_c} f_8\left(t,\ \epsilon\ (\cos\ \psi)/c\right). \tag{A.28}$$

Figure A-10 is a graph of f_8. The total short-circuit current is $i_{\ell sc}(t) = i_{\ell sc1}(t) + i_{\ell sc2}(t)$.

Open-Circuit Voltage - Transient Response to a Step Incident Field

By expanding $j \tan k_0 \ell$ in a power series of $e^{-j\omega(2\ell/c)}$, (A.14) can be written

$$V_{\ell 0c1} = \left[-E_0\, \epsilon\, f_5\left((g + \ell)/h,\ \Omega,\ k_0 h\right)\right]\left[1 + 2 \sum_{i=1}^{\infty} (-1)^i\, e^{-j\omega i(2\ell/c)}\right]. \tag{A.29}$$

The inverse transform of (A.29) is

$$V_{\ell 0c1}(t) = \epsilon E_0 \left[f_5\left((g + \ell)/h,\ \Omega,\ tc/h\right) + 2 \sum_{i=1}^{\infty} (-1)^i f_5\left((g + \ell)/h,\ \Omega,\right.\right.$$

$$\left.\left.(tc/h - i2\ell/h)\right) U(tc/h - i2\ell/h)\right]$$

$$= \epsilon E_0 f_7\left((g + \ell)/h,\ \ell/h,\ \Omega,\ tc/h\right). \tag{A.30}$$

Figures A-11 and A-12 are graphs of f_7 for various values of the parameters g/h and ℓ/h. For $\rho_g = -1$ and $\rho_\ell = 1$, (A.24) reduces to

$$v_{\ell 0c2}(t) = E_0 \epsilon (\cos\ \psi) f_9\left(t,\ (\epsilon \cos\ \psi)/c,\ \ell/c\right). \tag{A.31}$$

Figure A-13 is a graph of f_9. The total open-circuit voltage is $v_{\ell 0c}(t) = v_{\ell 0c1}(t) + v_{\ell 0c2}(t)$.

Sample Calculation

Problem: For the structure with the parameters listed below, find $i_\ell(t)$, $v_\ell(t)$, $i_g(t)$, and $v_g(t)$ at t = 5 nanoseconds for a 5-volt/m step electric field. The parameter values are:

$h = 3$ m, $a = 0.3$ m, $\epsilon = 0.01$ m, $a_1 = 0.001$ m, $\psi = 3\pi/4$,

$g = -1.5$m, $\ell = 1.5$ m, $Z_g = 540$ ohms, and $Z_\ell = 60$ ohms.

Solution: Calculate the following parameters for future reference:

$$Z_c = 120 \ell n[10 + \sqrt{99}] = 359.2 \text{ ohms}$$

$$\rho_g = \frac{2 \times 540 - 359.2}{2 \times 540 + 359.2} \approx 0.5$$

$$\rho_\ell = \frac{2 \times 60 - 359.2}{2 \times 60 + 359.2} \approx -0.5$$

$$g/h = -0.5$$

$$\ell/h = 0.5$$

$$(g + \ell)/h = 0$$

$$tc/h = 5 \times 10^{-9} \times 3 \times 10^{8}/3 = 0.5$$

$$\cos \psi = \cos (3\pi/4) = -0.707$$

$$\Omega = 2\ell n(2 \times 3/0.3) = 5.99.$$

From Figure A-2, $f_6(-0.5, 0.5, 0.5, -0.5, 6.0, 0.5) = 1.75$ and

$$i_{\ell 1}(5 \times 10^{-9}) = \frac{2 \times 5 \times 0.01}{359.2} 1.75 = 4.87 \times 10^{-4} \text{ amps.}$$

From (A.25),

$$f(5 \times 10^{-9}) = 5 \times 10^{-9} - 0.01/(3 \times 10^{8}) - [5 \times 10^{-9} - 0.01/(3 \times 10^{8}) - (-0.707) \times 0.01/(3 \times 10^{8})]$$

$$= -7.07 \times 10^{-3}/(3 \times 10^{8}) .$$

From (A.24),

$$i_{\ell 2}(5 \times 10^{-9}) = \frac{-[1 - (-0.5)] \times 3 \times 10^{8} \times 5}{359.2} [-7.07 \times 10^{-3}/(3 \times 10^{8})]$$

$$= 1.48 \times 10^{-4} \text{ amps} .$$

Then,

$$i_{\ell}(5 \times 10^{-9}) = i_{\ell 1}(5 \times 10^{-9}) + i_{\ell 2}(5 \times 10^{-9}) = 6.35 \times 10^{-4} \text{ amps}$$

and

$$v_{\ell}(5 \times 10^{-9}) = 60 \times i_{\ell}(5 \times 10^{-9}) = 3.81 \times 10^{-2} \text{ volts} .$$

From Figure A-1,

$$i_{g1}(t) = \frac{2E_0 \varepsilon}{Z_c} f_6\left(-(g + \ell)/h,\ \ell/h,\ \rho_{\ell},\ \rho_g,\ \Omega,\ tc/h\right)$$

and

$$f_6(0.0,\ 0.5,\ -0.5,\ 0.5,\ 6.0,\ 0.5) = 1.8 .$$

Therefore,

$$i_{g1}(5 \times 10^{-9}) = \frac{2 \times 5 \times 0.01}{359.2} 1.8 = 5.01 \times 10^{-4} \text{ amps} .$$

The current $i_{g2}(t)$ can be obtained from (A.24) by interchanging ρ_g and ρ_ℓ. For this problem

$$i_{g2}(5 \times 10^{-9}) = \frac{(1 - \rho_g)}{(1 - \rho_\ell)} i_{\ell 2}(5 \times 10^{-9}) = \frac{0.5}{1.5} \times 1.48 \times 10^{-4} = 4.93 \times 10^{-5} \text{ amps}$$

and

$$i_g(5 \times 10^{-9}) = i_{g1}(5 \times 10^{-9}) + i_{g2}(5 \times 10^{-9}) = 5.50 \times 10^{-4} \text{ amps} .$$

Then,

$$v_g(5 \times 10^{-9}) = 540 \times i_g(5 \times 10^{-9}) = 2.97 \times 10^{-1} \text{ volts} .$$

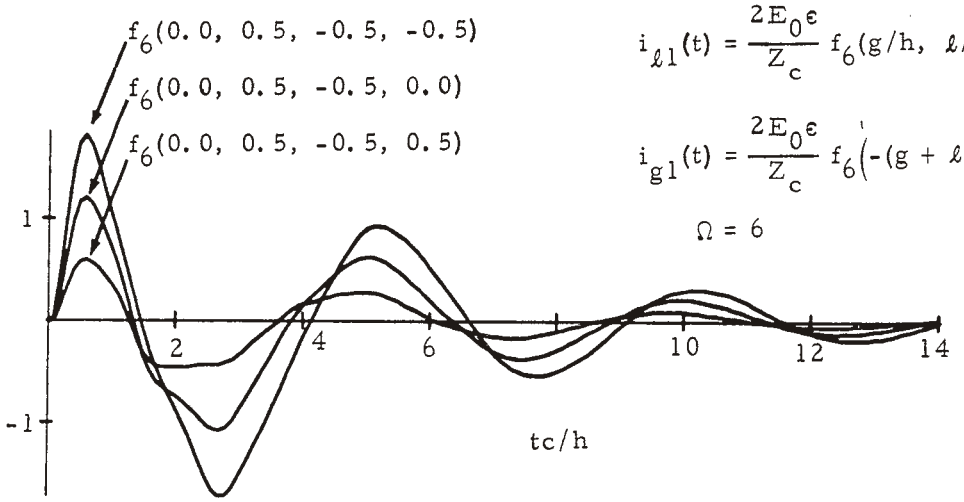

Figure A-1. Transient response to a step incident field.

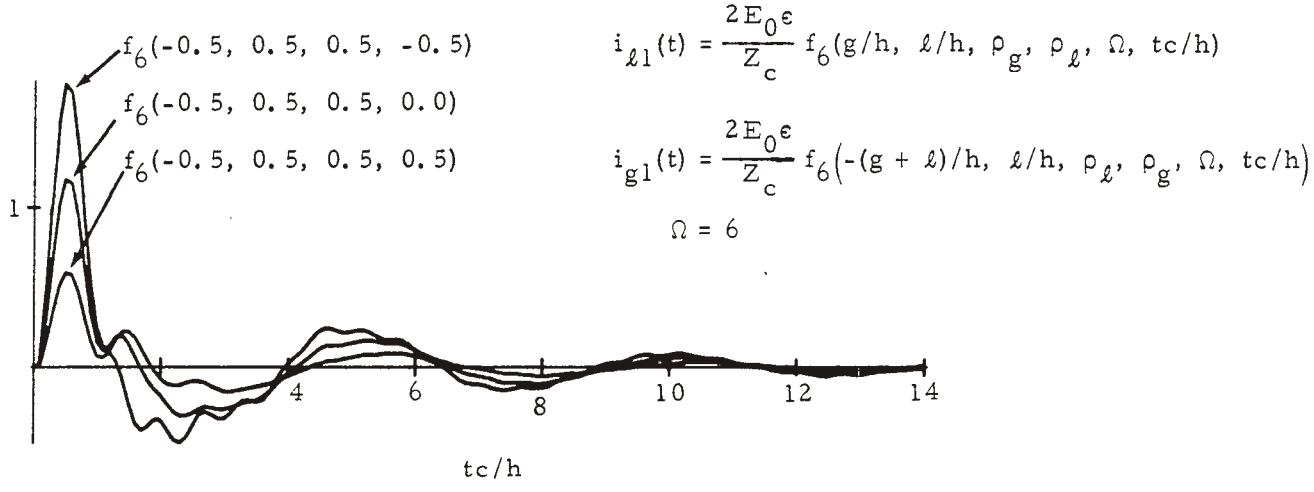

Figure A-2. Transient response to a step incident field.

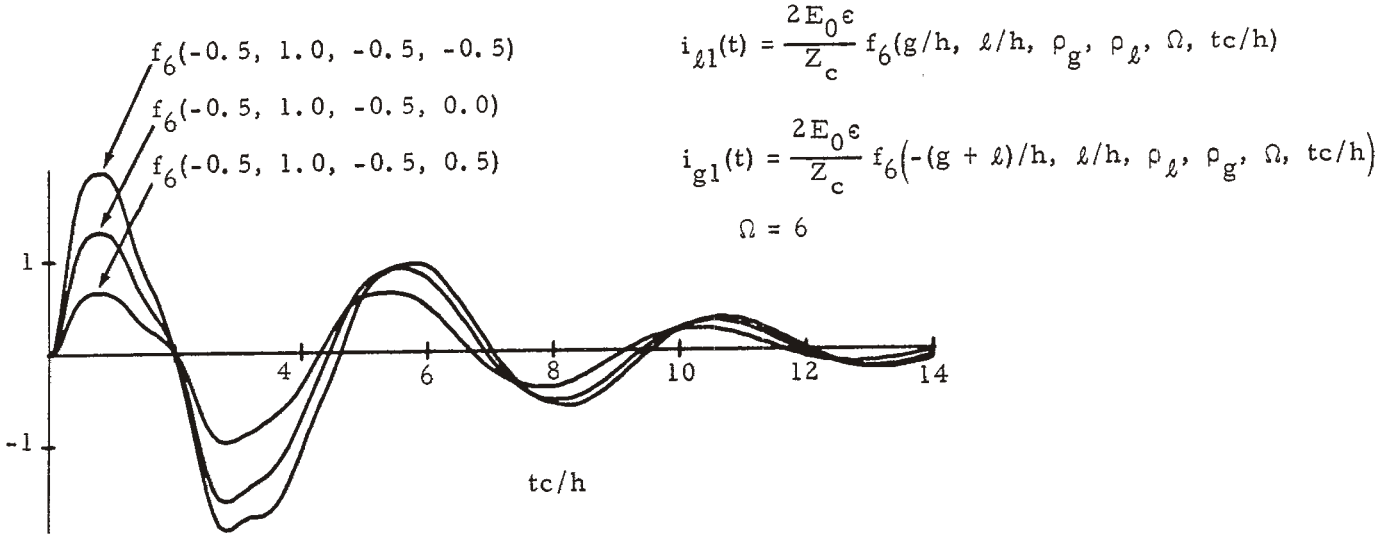

Figure A-3. Transient response to a step incident field.

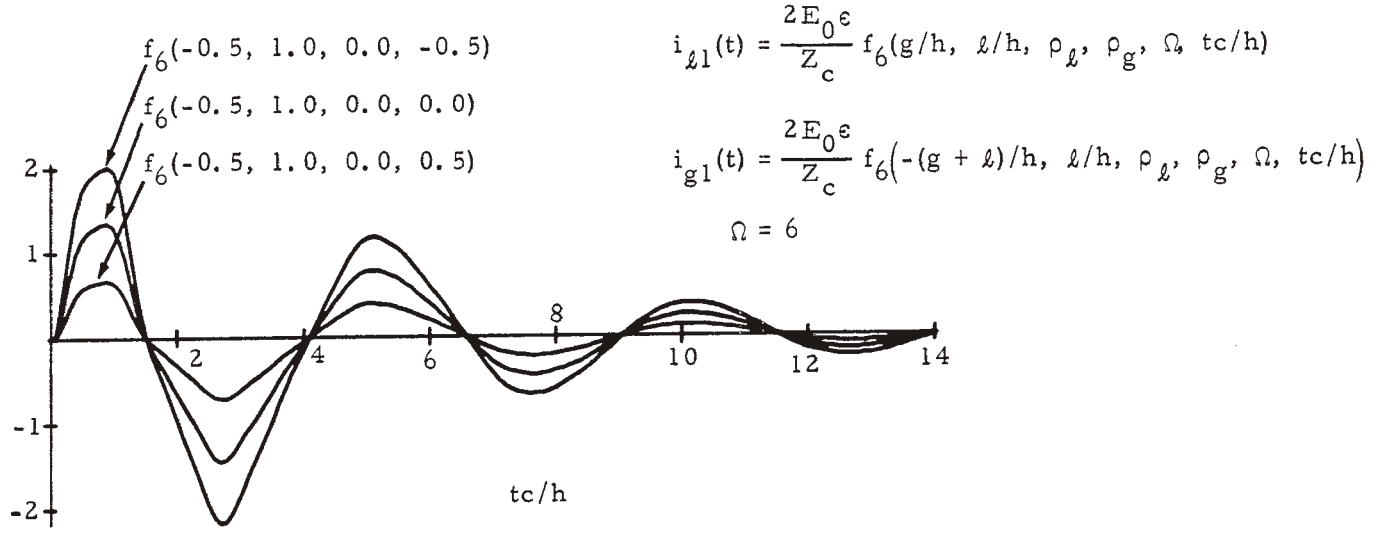

Figure A-4. Transient response to a step incident field.

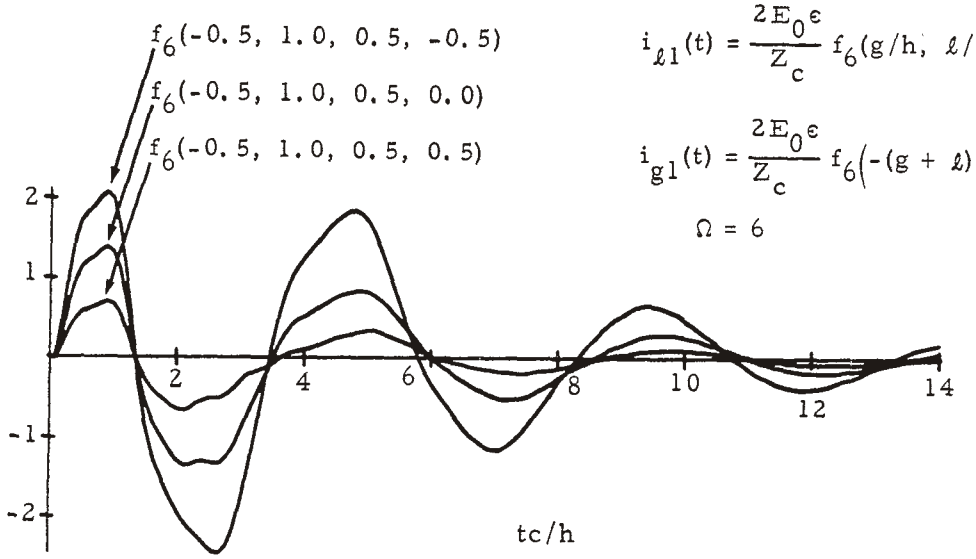

Figure A-5. Transient response to a step incident field.

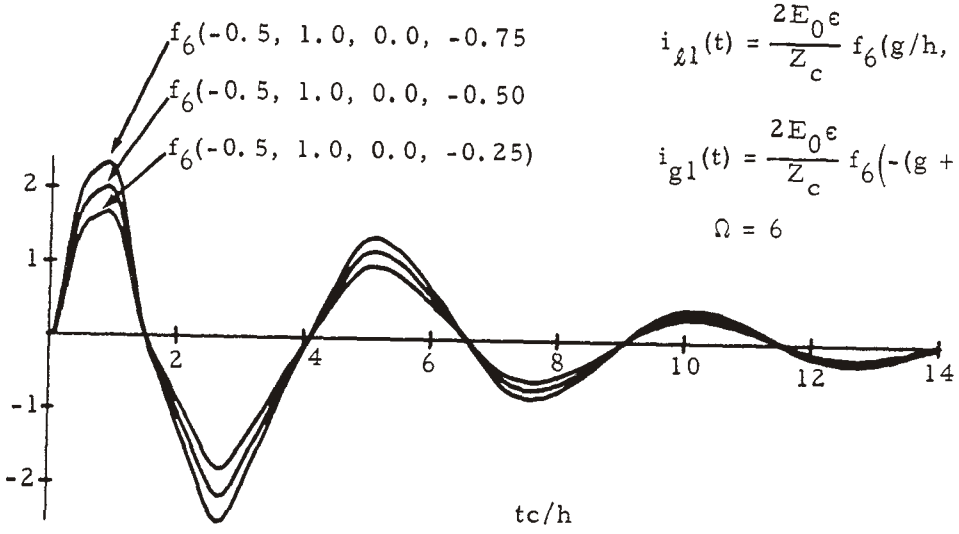

Figure A-6. Transient response to a step incident field.

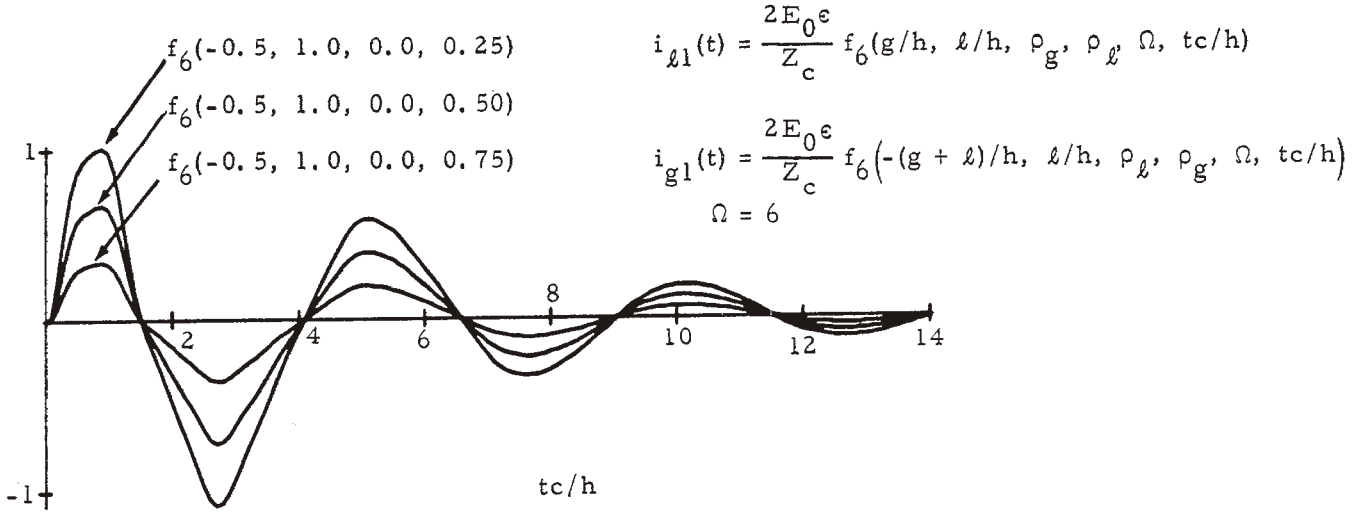

Figure A-7. Transient response to a step incident field.

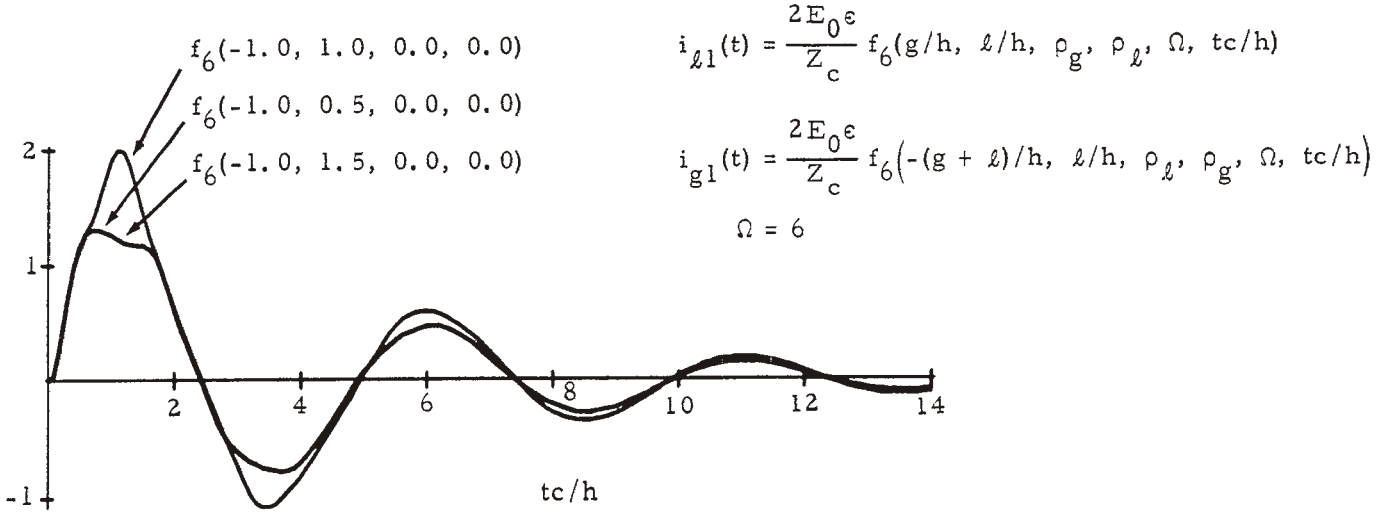

Figure A-8. Transient response to a step incident field.

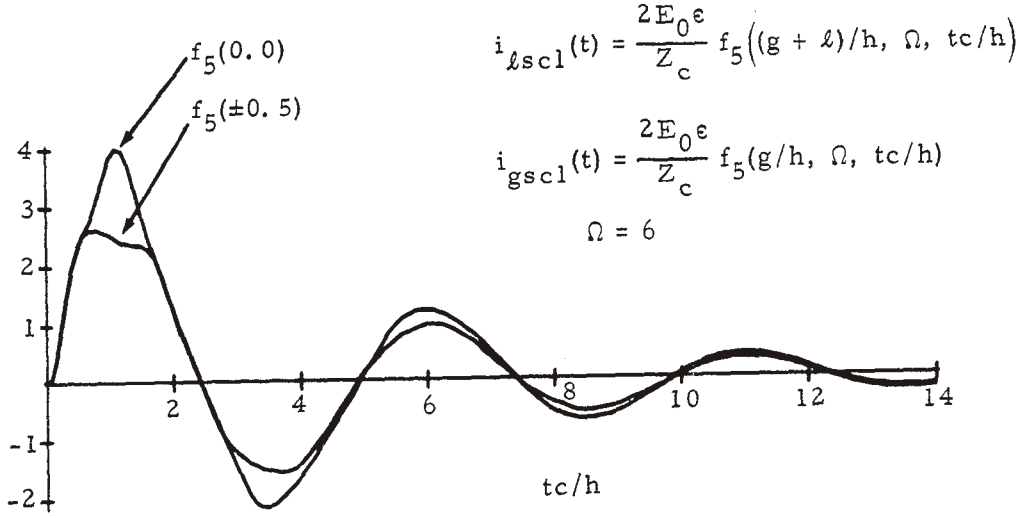

Figure A-9. Transient response to a step incident field (short-circuit current).

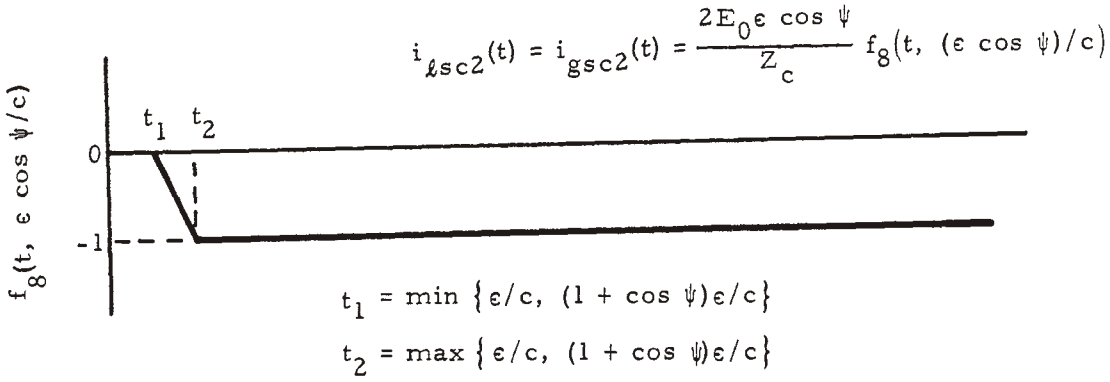

Figure A-10. Transient response to a step incident field (short-circuit current).

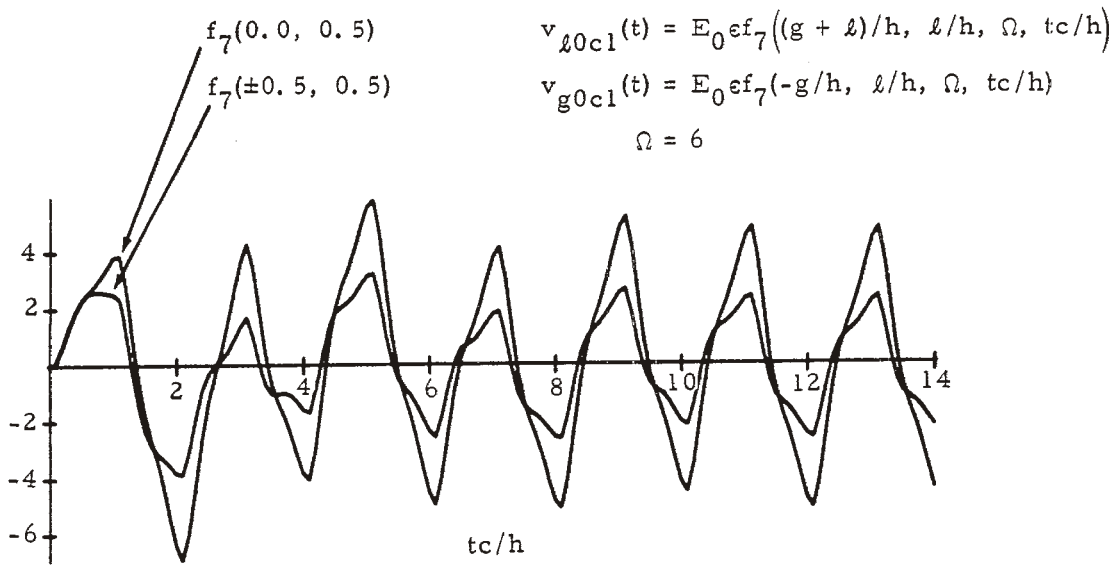

Figure A-11. Transient response to a step incident field (open-circuit voltage).

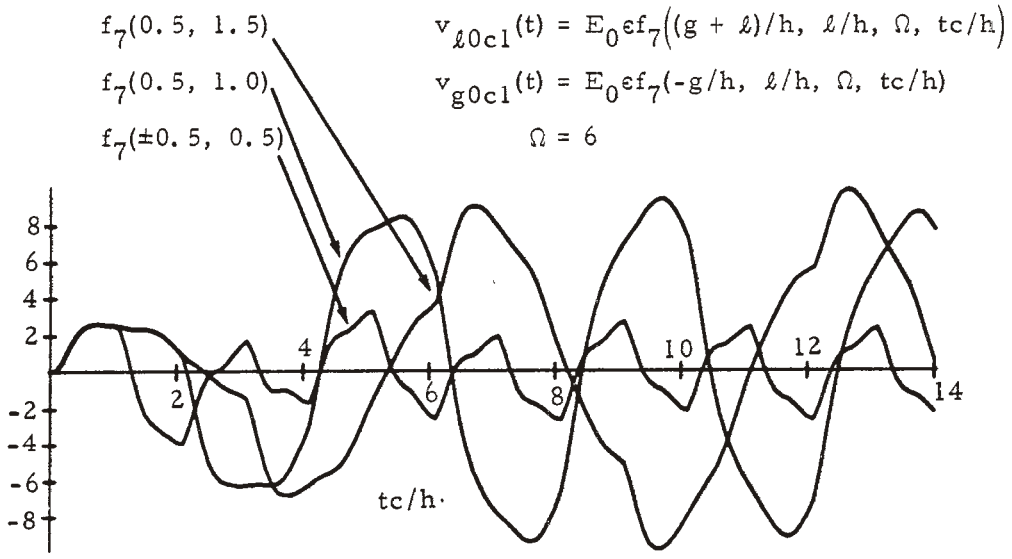

Figure A-12. Transient response to a step incident field (open-circuit voltage).

$$v_{\ell 0c2}(t) = v_{g0c2}(t) = (E_0 \epsilon \cos \psi)\, f_9(t, (\epsilon \cos \psi)/c, \ell/c)$$

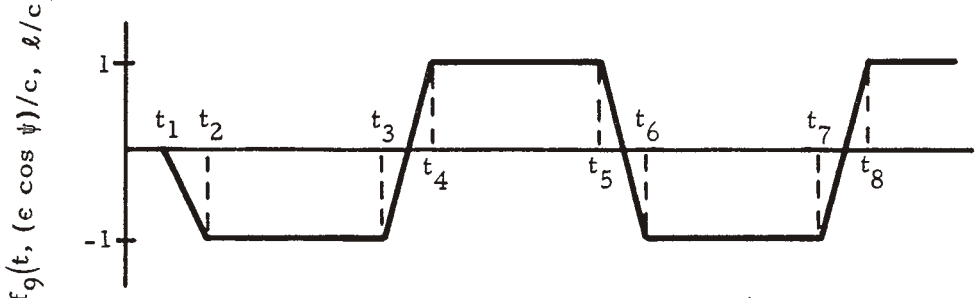

$$t_1 = \min\{\epsilon/c,\ (1 + \cos \psi)\epsilon/c\}$$

$$t_2 = \max\{\epsilon/c,\ (1 + \cos \psi)\epsilon/c\}$$

$$t_i = t_{i-2} + 2\ell/c;\ i = 3,\ 4,\ 5 \ldots .$$

Figure A-13. Transient response to a step incident field (open-circuit voltage).

REFERENCES

1. Harrison, C. W., Jr. (1967), "Response of transmission lines in proximity to a cylindrical scatterer," Radio Sci., 2 (9), 1083-1091.

2. Harrison, C. W., Jr., C. D. Taylor, E. E. O'Donnell, and E. A. Aronson, (1967), "On digital computer solutions of Fredholm integral equations of the first and second kind occurring in antenna theory," Radio Sci., 2 (9), 1067-1081.